APPLICATION OF RECENT ROTOR DYNAMICS DEVELOPMENTS TO MECHANICAL DRIVE TURBINES

by

William J. Caruso

Department Staff Engineer, Mechanical Research & Analysis

and

Bruce E. Gans

Senior Engineer, Bucket and Rotor Development

and

William G. Catlow

Manager, Bucket and Rotor Development

Mechanical Drive Turbine Department

General Electric Company

Fitchburg, Mississippi

William J. Caruso graduated in 1948 from Tufts University with a BSME degree. He also received an MSME degree from Northeastern University in 1970. He has been with the General Electric Company since 1948. His work has been concentrated in the design and development of rotating equipment.

Most of his activity has been in the fields of stress, vibration, materials, bearing lubrication, acoustics and shock. This activity has included steam and gas turbine bucket design, rotor dynamics, special low noise equipment for Navy submarines, vibration fatigue problems, rotor balance techniques and instrumentation.

His present position is Department Staff Engineer, Mechanical Research & Analysis, for the Mechanical Drive Turbine Department of the General Electric Company. He has published several technical papers and articles, and has been awarded four patents. He is a member of ASME and Tau Beta Pi and a registered professional engineer.

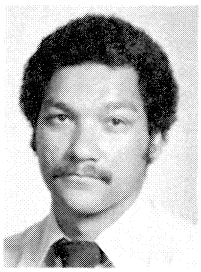

Bruce E. Gans is a Senior Engineer in Bucket and Rotor Development for the Mechanical Drive Turbine Department of the General Electric Company. He is involved in both vibration testing and analysis of turbine blades and rotors.

Mr. Gans has been with the General Electric Company for 11 years and has also been involved in turbine testing and design at GE Corporate Research and Development Center and at the Marine Turbine and Gear Department. He holds a B.S.M.E. degree from Rensselaer Polytechnic Institute, a M.S.M.E. degree from Northeastern University and is currently working on an Engineer's Degree in Mechanical Engineering at the Massachusetts Institute of Technology. He is also an ASME member.

William G. Catlow is Manager of Bucket and Rotor Development with the General Electric Company at the Mechanical Drive Turbine Department in Fitchburg, Massachusetts. He is responsible for development and testing of the steam turbine rotating components.

Mr. Catlow has had 13 years experience in turbomachinery, primarily in the areas of vibration, stress and thermodynamic analysis and testing. He holds a B.S. degree in Mechanical Engineering from Southeastern Massachusetts University and a M.S. degree in Mechanical Engineering from Worcester Polytechnic Institute. He is a member of ASME and past Chairman of the Worcester Section.

ABSTRACT

Recent developments in rotor dynamics technology are providing significant improvements in the correlation between theoretical analyses and actual rotor vibration response for mechanical drive steam turbines.

These developments involve analytical and experimental studies of tilting pad bearings, bearing supports, and steam force reactions.

The bearing analysis has been modified to include oil temperature, thermal gradient, and pressure loading effects which exist during normal operation. Pad pivot deflections, hot preload, and oil viscosity effects cause variations in the dynamic characteristics of the bearing. The resulting changes in the stiffness and damping coefficients are evaluated for the tilting pad bearings of a high speed turbine.

Bearing support structures, including special foundations, have been tested to determine their mechanical impedance as a function of frequency. The test results have been converted into analytical representations for use in the rotor dynamics analyses. The theoretical effects of dynamic support systems on the rotor vibration response are presented and compared.

Examples of typical steam turbine designs of different sizes and speeds have been analyzed, using the new concepts.

In each case, special response tests were conducted in which unbalance weights were installed in the rotor and the resultant changes in orbital vibration vectors were determined. The correlations between calculated and actual shaft amplitudes are shown for each case.

Bearing reactions are affected by directional steam forces which exist during turbine operation with partial arc steam admission. Recent analyses show the interaction of gravity and steam force vectors causing changes in the bearing oil film characteristics. This condition will not be evident in a routine no-load factory test, but may produce significant changes in rotor vibration for a turbine in service. Some field observations for turbines operating with load are presented to substantiate the analysis.

INTRODUCTION

Rotor Dynamics Background

Rotor dynamics technology as it exists today is the cumulative result of developments in each of the three major components of the total rotor dynamics system. The first of the components to be studied was the rotor. Rotor analysis began with the calculation of shaft fundamental natural frequencies by Rankine in 1869 [1]. A major milestone was the analysis of the vibration of a single disk due to an unbalance force by Jeffcott in 1919 [2]. For many years after this, however, the calculation of critical speeds was still limited to fundamental modes except for the simplest of rotors.

The modern era of rotor dynamics began in 1944 when Prohl developed a general method for calculating critical speeds of turbine rotors [3]. In that year, the same basic method, as applied to transverse beam vibration, was published by Myklestad as the result of an independent study [4]. For the first time, any rotor could be represented by a mathematical model that closely resembled the actual geometry. There was no need for the simplifying assumptions required by previous methods. The second and higher critical speeds and mode shapes could now be calculated as easily as the first. The iterative nature of the method lent itself to the use of large digital computers which were being developed. Within ten years, the critical speed program had been modified to add provisions for damping, asymmetric bearings and supports, and unbalance forces. The capability then existed for making calculations of synchronous rotor vibration response to added unbalance. The same general method is still being used for rotor analysis.

Analysis of the bearing component lagged the rotor analysis for many years. Some experimentally derived stiffness and damping coefficients became available in 1958 [5] but it was not until the mid-60's that the advent of high speed, high capacity computers made it practical to perform the theoretical analyses of bearing oil films without the need for many simplifying assumptions that were previously required [6] [7]. From that time on, there was remarkable progress in bearing analyses to more realistically represent the hydrodynamic oil film. Refinements and improvements continue to be made. An example of a recent development is described in this paper.

The stationary structure that supports the bearings is the third major component of the rotor dynamics system. The dynamic characteristics of the total support structure can have an appreciable effect on rotor response, depending primarily on the interactions between the oil-film coefficients and the dynamic stiffness of the supports.

The fact that rotor support flexibility reduced the first critical speed had been recognized for a long time. It was generally accounted for by static bearing deflections [8]. This concept was later extended to higher critical speeds, but produced large discrepancies in the prediction of actual critical speeds because of the omission of dynamic effects. To overcome this lack, the "dynamic stiffness method" was developed in 1958 [9]. This concept combined the bearing and support characteristics into equivalent dynamic stiffnesses as a function of rotor speed. The concept is still used in preliminary design work to produce "critical speed maps" that evaluate the dynamic compatibility between the rotor and its supports.

The development of new bearing analysis methods necessitated complementary developments in the bearing support area. Early attempts at mathematical analyses of supports were not successful in representing the complexity of the various connected structures that actually exist between the bearings and solid ground. As a result, mechanical impedance test procedures and equipment were developed [10] with which the dynamic characteristics of the total support structure were measured at the bearing interface. One of the recent developments in the application of mechanical impedance test data to rotor dynamics analysis is described in this paper.

Experimental Verification

Special rotor response tests are conducted in the factory in order to measure the orbital shaft amplitudes caused by unbalance weights and compare them to the calculated amplitudes for acceptable correlation.

The dynamic stiffness and damping characteristics of the bearings are confirmed in a special laboratory test facility which was developed for this express purpose. Measurements are made to define journal orbit motions for different types of bearings with various magnitudes of steady and whirling forces applied. The journal can be run at any speed up to 4500 rpm and the test section can accommodate a 7 inch diameter bearing. The magnitude and direction of the steady force is controllable as well as the magnitude of the whirling force. The desired Sommerfeld and Reynolds numbers are obtained by suitable combinations of oil viscosity and bearing load.

The shaft orbits predicted by the bearing analyses, using calculated stiffness and damping coefficients, are compared to the orbits determined by test. The correlation between them is a measure of the accuracy of the calculated coefficients. As a consequence of the laboratory test results, the basic analytical bearing model has been modified to include the effects of local elastic deflections of tilting pad contact surfaces, thermal distortions of pads, and fluid inertia.

The dynamic characteristics of the bearing supports are derived from impedance tests which are made on fully assembled turbines. The turbines are installed on special test foundations which are intended to simulate the relatively massive, reinforced concrete structures typical of field installations. The same special factory test foundations are also used for the rotor response tests.

Practical Application

The basic design philosophy for rotors, bearings, and supports is to consider the effects of each on the vibration response of the total rotor dynamics system. Rotors are designed to be stiff relative to the bearings. Shaft end overhang lengths and coupling weights are minimized. Bearing supports are designed to be stiffer than required for mechanical or alignment considerations. Bearing type, size, and clearance are selected because of the dynamic oil film characteristics as well as for losses, oil flows, and temperature rises.

Because so many design decisions are based on rotor

dynamics analyses, it is extremely important that the validity of the calculated responses be established. This can only be done for the total rotor dynamics system by accurate response testing of complete turbines. The emphasis is on measurement of absolute shaft motions so that orbital amplitudes may be directly compared to calculated values.

As more sophisticated analyses are developed and applied, the effects of the various components in the system can be segregated with more certainty. A better understanding of component effects will emphasize areas in which design modifications can be made to reduce rotor response.

BEARING ANALYSIS

The usual analysis used for calculating stiffness and damping coefficients of journal bearings includes simplifying assumptions such as:

1. Journal pads are infinitely stiff in the radial direction.
2. Pad contours and bearing clearances are not affected by operating conditions.

Recent developments outlined below are used to evaluate a bearing's dynamic properties with more realistic conditions.

Hertzian Effects

The assumption that the pad is infinitely stiff has a significant effect on a bearing's stiffness and damping coefficients [11] [12]. The local elastic deflection at the pad contact point due to Hertz stresses acts as a spring combined with the oil film stiffness and damping characteristics, as shown in Figure 1. This additional flexibility reduces the effective stiffness and damping of each pad and therefore of the entire bearing. It is important to note that special account should be taken for the various bearing pad pivot designs. The pivot configuration and contact profile can have a significant impact on the stiffness and damping contribution from the Hertzian effect. For example, line contact pivots are stiffer than point contact pivots.

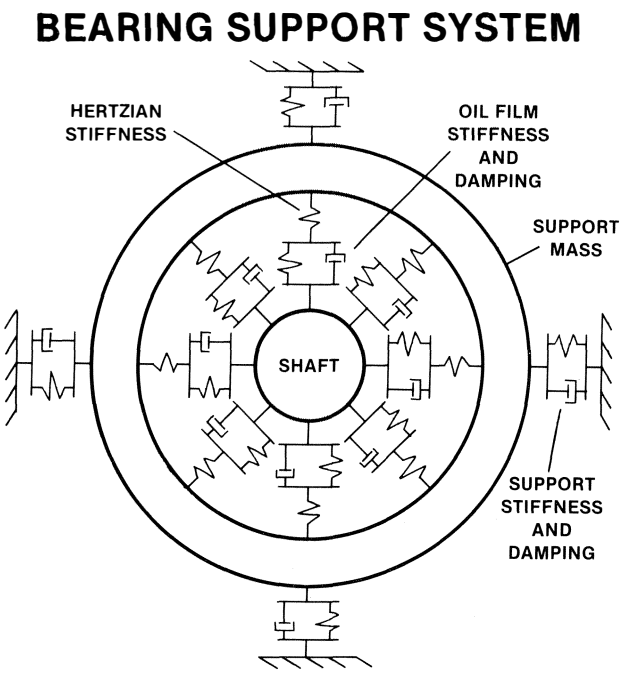

Figure 1. Schematic Sketch of Bearing Oil Film and Bearing Support Stiffness and Damping Model.

A common practice for including the Hertzian effect has been to reduce the total stiffness values assumed for the bearing supports. Having calculated the oil film characteristics, the total bearing support stiffnesses could be derived by adjusting them until the calculated response to unbalance curve correlated with measured data. This calibration is lost when either the bearing type or bearing supports are changed. To properly account for Hertzian deflection, the stiffness and damping coefficients must be determined for each particular pivot geometry in addition to journal and pad geometry. Standard published data for oil films cannot be used directly. The interaction of pivot flexibility and the oil film is more complex than simply adding an additional stiffness in series with the unmodified bearing data. Figure 1 simplistically shows the Hertzian stiffness in series with oil film stiffness and damping coefficients. When the Hertzian deflections are considered in the analysis, all of the oil film coefficients will be modified because the deflected pad changes the position of the journal relative to the other adjacent pads.

Besides pivot configuration, considerable variation is found in the characteristics of tilt pad bearings depending on how the pivot is physically attached to the pad. Some pad designs have the pivot integral with the pad. For such configurations a calculated Hertzian deflection will result in accurate stiffness predictions. Other designs have one or more shims between the pivot and the pad to enable better dimensional control of bearing clearances. These pieces are not all in theoretically perfect contact because of surface finish, surface films, or slight deviations in the contours of mating surfaces. Under these conditions, the stiffness characteristics are reduced from the theoretical Hertzian value (see Figure 2). This is a significant effect in further reducing stiffness and damping of the bearing. On such assembled tilting pad designs the load-deflection characteristic must be experimentally determined and included in the bearing analysis.

Hot Preload

There are thermal effects which occur in operation due to

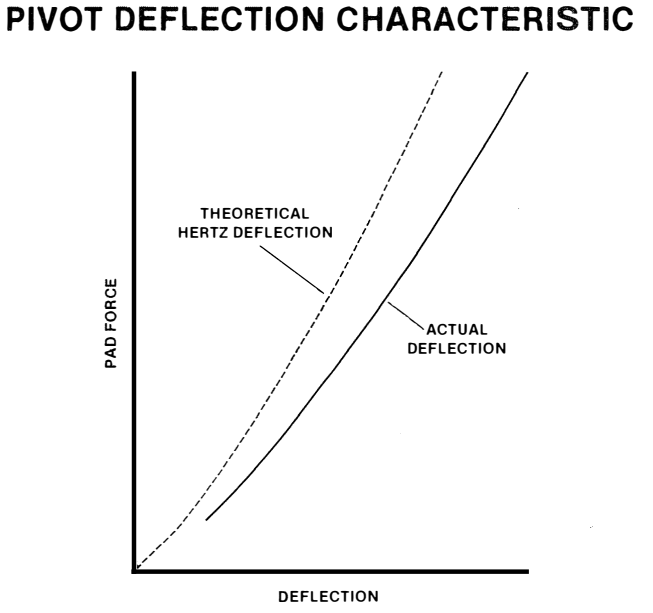

Figure 2. Comparison of Theoretical and Actual Force-Deflection Characteristic for Non-Integral Tilting Pad Pivot Construction.

differences in temperature of the various components as shown in Figure 3. The actual running clearance is reduced because the shaft and pads are hotter than the bearing housing. In addition to the slight decrease in clearance, the temperature gradient across the pad causes an increase in the pad's radius of curvature. The net effect is to create preload at operating conditions even though the rotor/bearing combination was initially assembled with zero preload.

The radii of pads in the bearing lower half increase slightly due to bending from static pressure considerations. Estimates can be made of this change by applying appropriate pressure distributions on the pad. The total hot preload is the result of both thermal and pressure distortions during normal operation. The hot preload for a typical 5 LBP (5 pads, with load between pads) bearing used in a turbine with a maximum operating speed of 11,000 rpm is shown in Figure 4. The preload has been calculated based on actual measured pad temperature data and, as shown, can be significant. The preload ratio is defined as the "assembled clearance" divided by the "machined clearance". For a nominal design preload of zero, the preload ratio equals 1 and the assembled clearance is equal to the machined clearance. In operation, the hot preload is the result of a slight decrease in the assembled clearance and an increase in the pad radius as machined. This is the ratio shown in Figure 4, labelled "as modified in operation". For a bearing design, with a nominal zero preload, the machining tolerances for journals, pads and bearing housings can accumulate in extremes to produce either positive or negative preload. The magnitude, however, is less than the hot preload value and the bearing will always run with some amount of positive preload.

Oil Viscosity

Another effect that influences the dynamic characteristics of tilting pad journal bearings is the change in oil viscosity with oil film temperature. The oil film temperature may be derived from journal pad temperature measurements. [13] Figure 5 shows how the pad temperature increases with speed. Journal-bearing thermocouples are typically located on the loaded pad

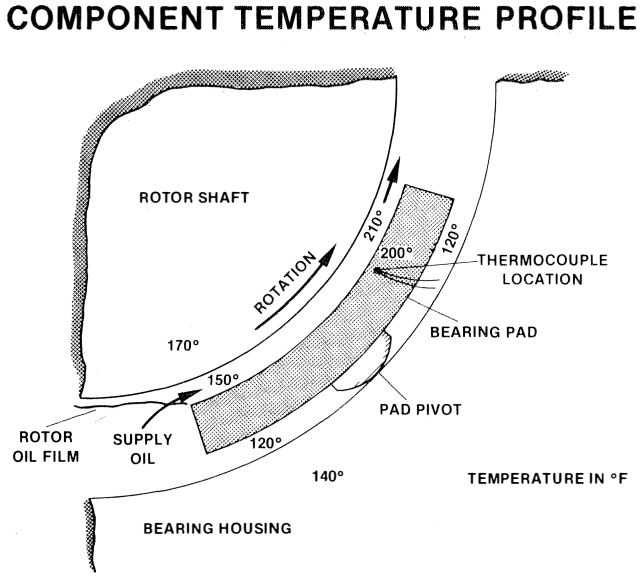

Figure 3. Operating Temperature Profile of Elements of High Speed Turbine Bearing.

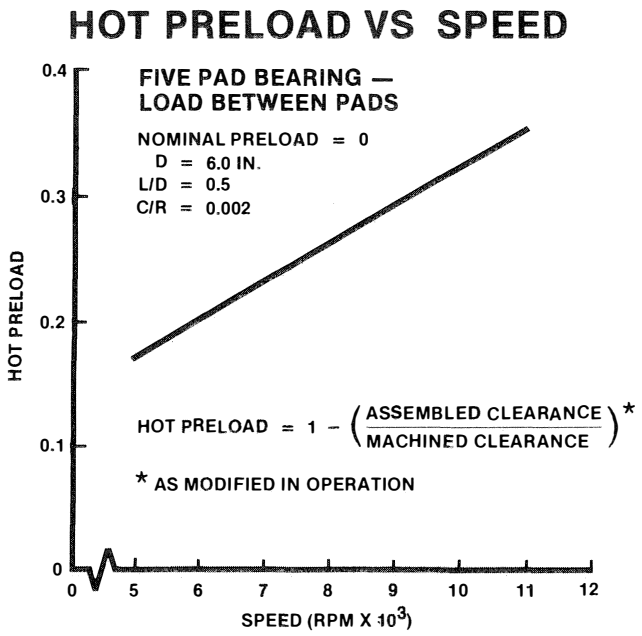

Figure 4. Variation of Hot Preload with Shaft Speed for High Speed Turbine.

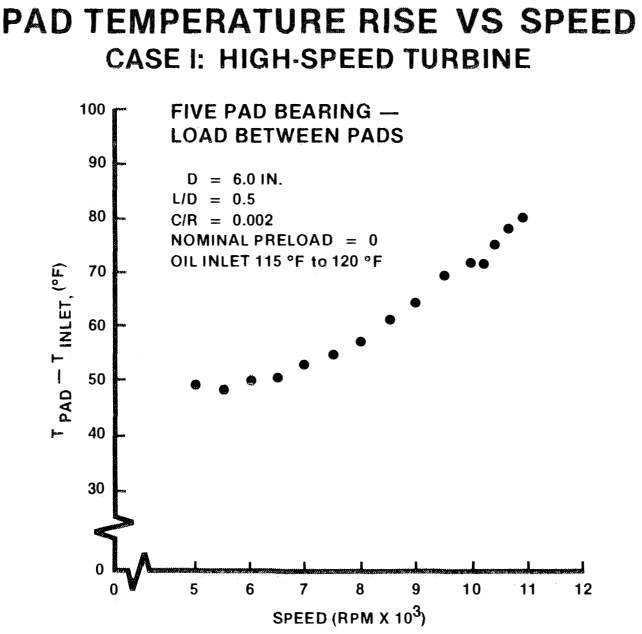

Figure 5. Variation of Pad Temperature with Shaft Speed for High Speed Turbine.

toward the pad trailing edge where the minimum oil film thickness is expected. The actual local oil film temperature is higher than the measured pad temperature and can be estimated from heat balance considerations. It is necessary to know how the oil film temperature varies along the load pads in order to establish a realistic oil viscosity. This is a complex heat transfer problem. The oil entering each pad is not at supply temperature but at an intermediate value due to the mixing of cooler supply oil and the hotter oil film adhering to the journal. An increasing oil temperature along the pad, as shown in

Figure 3, can be assumed when calculating stiffness and damping coefficients.

Dynamic Coefficients

Figures 6 and 7 illustrate changes in the direct stiffness and damping coefficients for a particular bearing when the above effects are considered, as compared to the results of conventional calculations. (The cross-coupling terms for the tilting pad bearing are extremely small relative to the direct terms and are of very little significance in the analysis.) The relative significance of the different effects will vary depending on the specific applications. To improve the agreement in the prediction of turbine resonances with respect to location and amplitude all of these effects should be included in the calculation procedure, since it may not be known prior to initial calculation which are the most significant. This is consistent with the observation that the resultant change in rotor response is a function of the total system and cannot be predetermined with any certainty by consideration of the bearing characteristics alone.

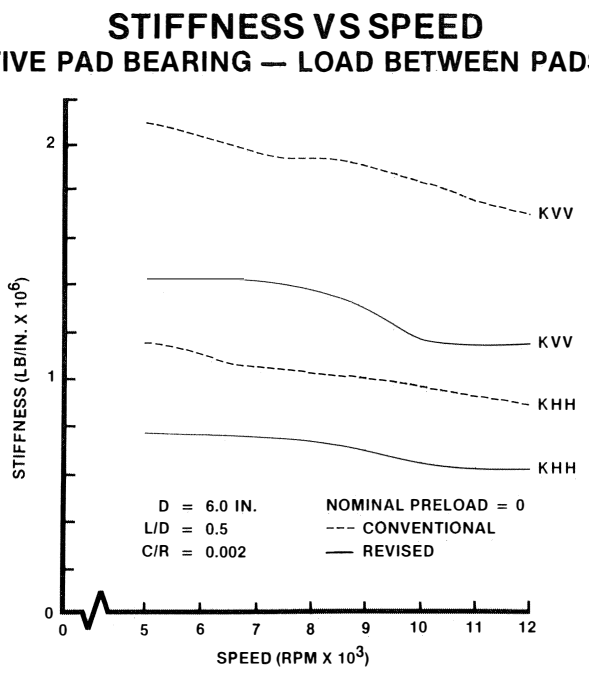

Figure 6. Comparison of Stiffness Coefficients for Conventional and Revised Bearing Models. KVH and KHV not Shown Because the Values are Very Low.

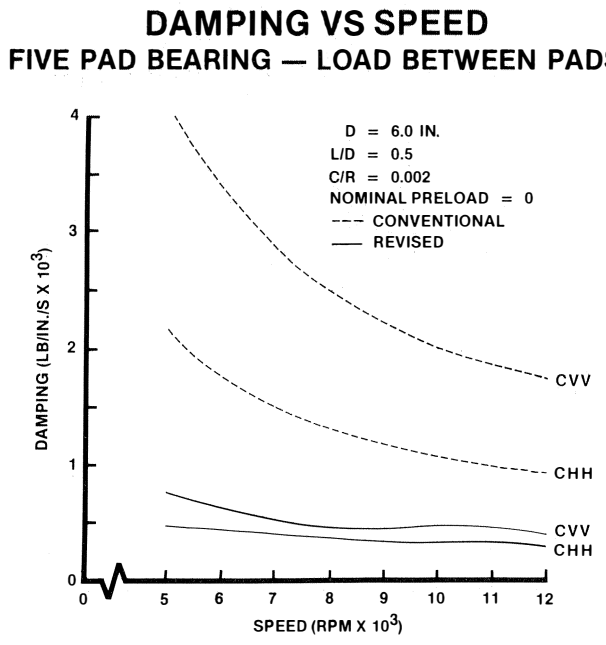

Figure 7. Comparison of Damping Coefficients for Conventional and Revised Bearing Models. CVH and CHV not Shown Because the Values are Very Low.

BEARING SUPPORTS

The dynamic characteristics of the structure that supports the bearings can have an appreciable effect on rotor response. The support theoretically includes all of the mechanical elements installed between the oil film and the earth. Part of this is a function of the turbine design; the other part is in the foundation design.

Turbine Components

The turbine casing support at the thrust bearing end of the turbine is usually a flex-plate design as shown in Figure 8. It accommodates axial thermal expansions by bending, but is stiff in the vertical and transverse directions. The flex-plate component is a weldment with provisions for bolting to the bearing housing and to the foundation sole plate.

The bearing support at the drive end of condensing turbines includes the exhaust casing wall and the integral casing support feet. The support feet are free to move transversely to accommodate casing thermal expansions, and they are keyed to resist axial movement. Considerable design effort has been made to achieve increased stiffness in the transmission path from the drive end bearing, through the back wall, and into the casing support feet.

One of the important reasons for maximizing stiffness between the bearings and the foundation is that it optimizes the inherent damping characteristics within the bearing oil film due to the relative motion between the journal and the bearing.

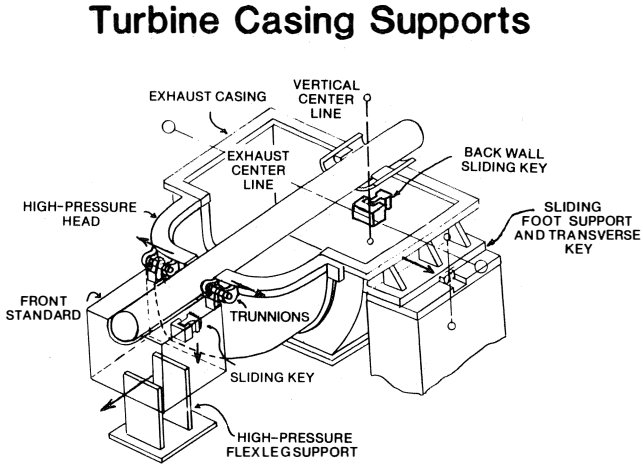

Figure 8. Casing Support Construction for Typical Condensing Turbine. Flex Plates at High Pressure End, Supports Integral with Casing at Low Pressure End.

Foundations

The most common foundation designs are relatively massive, reinforced concrete structures that present a high impedance to the turbine at the connection points. In this respect, they are dynamically similar to the special bases that support the turbine during vibration response tests run in the factory. The experience has been that the factory test results have been predictive of subsequent operation in the field.

Impedance Testing

The total bearing support structure is complex. Thus, its dynamic characteristics are difficult to represent and analyze with a complicated mathematical model. In the past, reasonable correlation was obtained between rotor dynamics analyses and unbalance vibration response tests when a simple approximation of support stiffness was used.

The support stiffness was based on static deflection, either measured or estimated. In a later development, the dynamic characteristics of turbine bearing support structures were determined by impedance testing. In these tests, an alternating force of variable frequency is applied to a location on the structure and the resulting vibratory motion is measured at the same point and in the same direction. The ratio of the force and vibration vectors is referred to as the direct or driving point impedance. Any one of several different ratios can be used to dynamically characterize a structure. Ratios of force to acceleration, velocity, or displacement are respectively defined as Dynamic Mass, Mechanical Impedance, or Dynamic Stiffness. The test data has been obtained in terms of Mehanical Impedance.

Since the ratios are related to each other by frequency, a single plot of Mechanical Impedance vs. Frequency will also display Dynamic Stiffness and Mass.

Various types of equipment are commercially available to perform impedance testing. An electrohydraulic inertial mass force system has been successfully used to test turbine bearing support structures as shown in Figure 9. It is capable of developing an alternating force of 1000 lbs., peak-to-peak, over a frequency range from about 30 to 300 Hz. The physical size of the shaker (55 lbs. inertial mass) is compatible with the size and mass of the turbine structures. The shaker force is capable of producing sufficient motion so that transducer sensitivity is not an issue. At the same time, the shaker is small enough to fit within the bearing bracket so that the measured impedance is close to what the rotor system will experience.

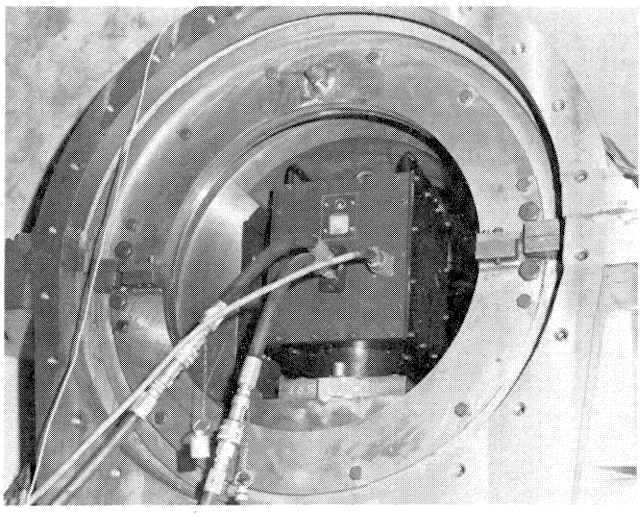

Figure 9. Hydraulic Shaker Mounted Within Low Pressure End Bearing Housing of Large, Medium Speed Turbine. Vibratory Force is Applied in Vertical Direction.

In addition to measuring the direct or driving point impedances, transfer impedances were also measured. A transfer impedance is the ratio of the driving force at the bearing to the motion at another location on the structure or in a different direction than the driving force. Transfer impedances from one bearing support to the other were measured, as well as the cross impedance from the driving force at a point to the motion normal to the driving force direction at the same point. In both cases, the general level of these transfer impedances was substantially greater than the direct impedances.

This provided a simplification of the bearing support since cross-coupling effects could be neglected and each bearing support could be considered independent of the other.

A typical impedance plot is shown in Figure 10 for the drive end bearing support of a turbine. The exciting force was applied at the bearing location in the vertical direction, and the motion was measured at the same location and in the same direction. The ratio of driving force to vibration velocity is the direct or driving point impedance.

The ordinate scale is the mechanical impedance ratio which is pounds of force divided by velocity in inches per second. The abscissa is frequency in Hertz. The diagonals which slope downward to the right are dynamic stiffness ratios

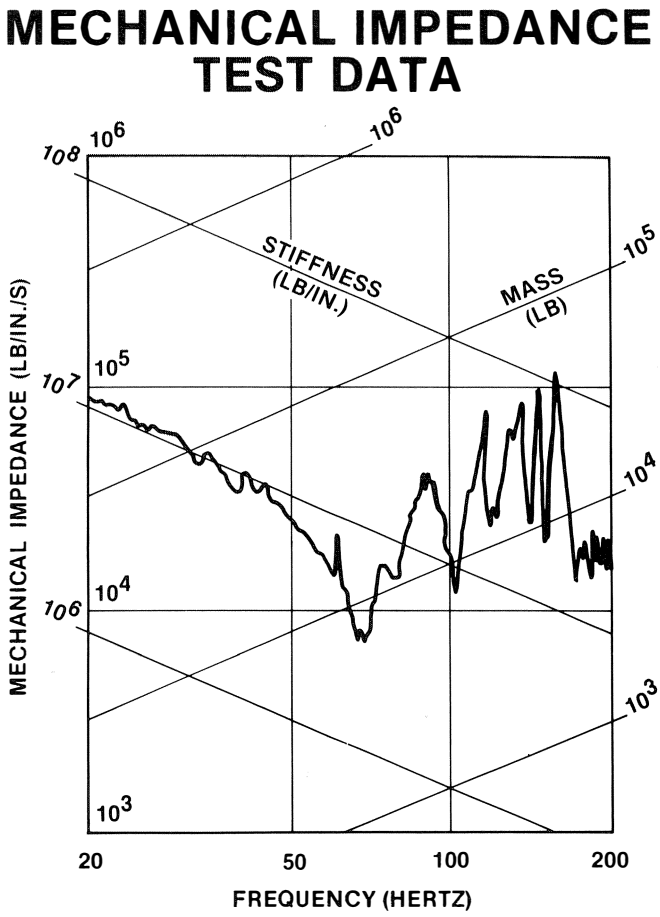

Figure 10. Direct Impedance Data for Low Pressure End Bearing Support of Large, Medium Speed Turbine, in Vertical Direction. Valleys Indicate Damped Resonances.

which are pounds of force divided by amplitude in inches. The diagonals which slope upward to the right are effective mass lines in pounds of weight. Each valley in the impedance plot is a resonant frequency, and each peak is an antiresonant frequency. At the resonant frequencies, the supporting structure presents a lower impedance (dynamic stiffness) to the rotor bearing, oil-film system at the interface between them. This means that the unbalance force transmitted from the rotor will cause an increase in bearing bracket amplitude at that frequency. The opposite is true at the antiresonant frequencies. In this case, the dynamic stiffness at the bearing bracket is high, which results in a decrease in bracket amplitude due to rotor unbalance forces. The mechanical impedance at the bottom of each valley is the system damping at that frequency. The nearly constant dynamic stiffness at low frequencies extends to the static stiffness value.

Mathematical Representations

The first use of the impedance test data was to derive average dynamic stiffness values for applicable frequency ranges. It was determined, however, that the effects of mass and damping should be included, as well as stiffness. Accordingly, simple spring-mass-damper models are now being used to simulate the impedance test results for different discrete speed ranges.

The mechanical impedance data of Figure 10 is replotted in Figures 11 and 12 as dynamic stiffness vs. operating speed.

In Figure 11, the general variation of dynamic stiffness with speed is approximated by lines of constant stiffness within discrete speed ranges. Figure 12 illustrates the use of different spring-mass-damper models within discrete speed ranges where major resonances occur. The calculated dynamic stiffnesses of the simple models simulate the actual impedance data as shown by the dashed lines in Figure 12.

In the past, it was recognized that, in many cases, the effects of bearing supports had to be included in the rotor dynamics analysis in combination with the bearing oil film characteristics. The concept of a rigid or extremely stiff support is not valid from a realistic standpoint but such an assumption has provided reasonable correlations between calculated and test responses when the bearing oil film was flexible relative to the support. In these cases, the oil film characteristics dominated the system response and it didn't make much difference whether or not the support stiffness was included in the analysis. In many other cases, however, the correlation was improved by representing the supports by simple vertical and horizontal springs having the same static stiffness value for both bearing supports in both directions.

Impedance testing provided a greater insight into the dynamic behavior of different supports and provided more realistic stiffness values for vertical and horizontal directions.

A more recent development is the representation of each bearing support in the vertical and horizontal directions by different spring-mass-damper models to simulate actual impedance data within discrete speed intervals over the entire speed range. Figure 13 shows the differences in calculated response for a large, medium speed turbine due solely to the manner in which the bearing supports were represented. The bearing oil film coefficients have been calculated as described in Section II. The unbalance is added to the LP (low pressure shaft end) drive coupling. The shaft amplitude near the adjacent LP bearing is plotted. The "constant stiffness" response curve was calculated using a constant stiffness value of 6 x 10^6 lbs./in. in the vertical and horizontal directions for the HP (high pressure end) and LP bearing supports. The "springs only" response curve was calculated using stiffnesses which

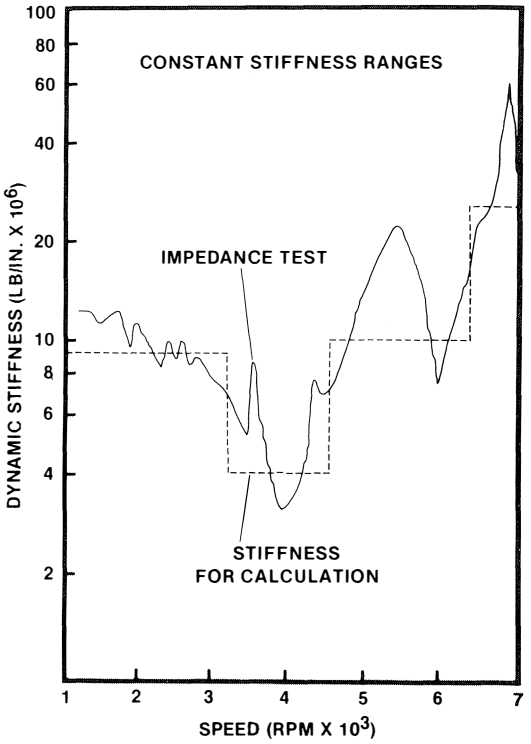

Figure 11. Mechanical Impedance Test Data from Figure 10, Replotted as Dynamic Stiffness vs. Speed. Horizontal Dashed Lines are Stiffnesses Used in Response Calculations.

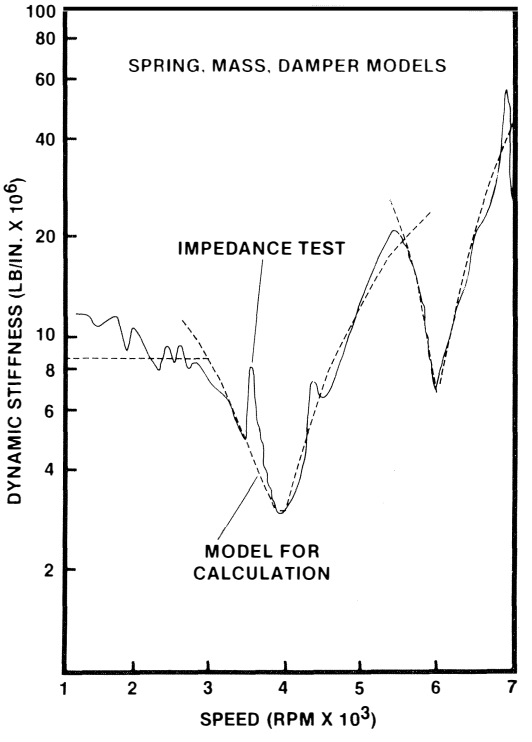

Figure 12. Mechanical Impedance Test Data from Figure 10, Replotted as Dynamic Stiffness vs. Speed. Different Spring-Mass-Damper Models Used for Discrete Speed Intervals in Response Calculations Produce Stiffnesses Shown by Dashed Lines.

varied in accordance with the general variations in the dynamic stiffness as derived from impedance testing. For example, Figure 11 shows the stiffness values for the LP support in the vertical direction. Table 1 lists stiffnesses and applicable speed ranges. Note the substantial difference in Figure 13 between the "springs only" curve and the "constant stiffness" curve. This is unexpected in view of the fact that the stiffness values in both calculations are the same order of magnitude. It should be noted, however, that the direct stiffnesses of the bearing oil films are between 3 x 10^6 and 4 x 10^6 lbs/in. over the speed range. The interaction with the supports, therefore, has a significant effect.

The third curve in Figure 13 is the response curve when each bearing support is represented, in the vertical and horizontal directions, by simple spring-mass-damper models within different speed ranges.

The comparisons between calculated and test responses are shown in Figures 14, 15 and 23.

The three support configurations were evaluated for HP and LP bearing locations in terms of correlation between calculated and test responses. The constant stiffness supports produce reasonable correlation at the LP bearing but not as good at the HP bearing. When the support impedances are represented by springs alone, the correlation is poor at both bearings. With spring-mass-damper models, the correlation is reasonably good at both bearings.

TABLE 1. SUPPORT STIFFNESS RANGES.

	K x 10^6 lbs/in	Speed, RPM
HP Bearing:		
Vertical	2.0	0-3900
	4.0	3900-6900
Horizontal	5.0	0-3750
	10.0	3750-5200
LP Bearing:		
Vertical	9.0	0-3250
	4.0	3250-4550
Horizontal	2.5	0-2850
	3.5	2850-4050

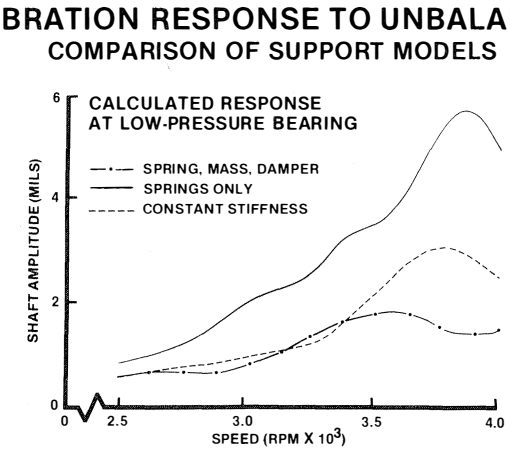

Figure 13. Comparison of Responses Using Different Representations of Bearing Supports. "Springs Only" and "Spring-Mass-Damper" Models Derived as in Figures 11 and 12. "Constant Stiffness" Model is Spring with 6 x 10^6 lbs./in. Stiffness in Both Directions at all Speeds. Bearing Oil Film Coefficients are the Same for all Three Curves.

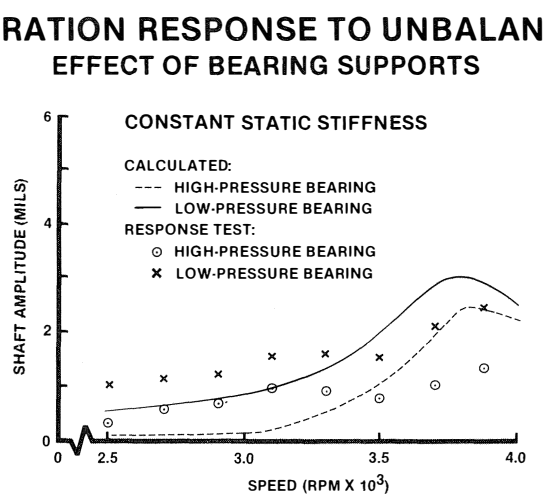

Figure 14. Response Correlation for Large, Medium Speed Turbine Using 6 x 10^6 lbs./in. Constant Stiffness for Bearing Supports in Both Directions and for all Speeds.

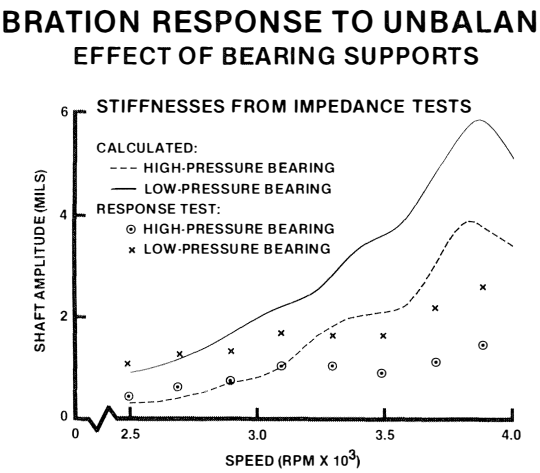

Figure 15. Response Correlation for Large, Medium Speed Turbine Using "Springs Only" Stiffnesses for Bearing Supports Derived as in Figure 11 and as Listed in Table I for Different Directions and Speeds.

Field Test

It has been shown that the bearing supports can have an influence on rotor response. The total bearing support has two major components: the turbine structure and the foundation. In the analysis, the components are combined into one representation of the total support which includes the factory test foundation. To minimize the effect of the factory test foundation on rotor response, the test pedestals are designed to be as massive and rigid as practical. They are steel, concrete-filled, structures which extend beyond the actual turbine supports and have minimum heights above the steel factory floor compatible with the test facility piping access requirements.

The overall experience with turbines in service indicates that typical, reinforced-concrete turbine-compressor decks in the field are probably dynamically similar to the factory test

foundations. This is primarily based on observations of first critical speeds and the general behavior of operating turbines. There have not been any opportunities to actually conduct rotor response to unbalance tests in the field for direct comparison with factory tests. Recently, however, a rotor balance operation was performed on a high speed turbine in service, during which a trial weight was installed in a mid-span balance plane. Vibration data was obtained at three different speeds within the operating range. This turbine had previously been response tested in the factory with unbalance added in the same mid-span plane. The comparison between factory and field response for the same amount of added unbalance is shown in Figure 16. The correlation between the factory and field tests is extremely close at the three balance speeds and the trend of the vibration amplitudes with speed is the same for both tests. This is verification that, in this case, the actual foundation component of the total bearing support did not significantly affect total rotor response as measured using the factory test foundations.

ROTOR VIBRATION RESPONSE TO UNBALANCE FORCES

Design Analysis

Normally, when the total rotor lateral vibration analysis is performed, the number, size and location of the stages, and the bearing span have been established by application and efficiency requirements. This leaves changes in bearing type and size, shaft diameters and shaft end overhangs to improve lateral response characteristics. These characteristics include shaft resonant speeds, and response to unbalance. The basic design philosophy is to avoid rotor criticals in the operating speed range, if practical, and provide sufficient damping in the system to make the rotor insensitive to unbalance. With a rotor design that is relatively stiff, the influence of changes in shaft diameters does not significantly change the critical speed locations. This is particularly true for first criticals. Second and third criticals are influenced by the amount of overhung weight at the coupling end. The effect of overhung weight can be minimized by bringing the coupling as close to the bearing centerline as possible, minimizing the use of adapters between the coupling and the shaft, and minimizing the weight of the coupling.

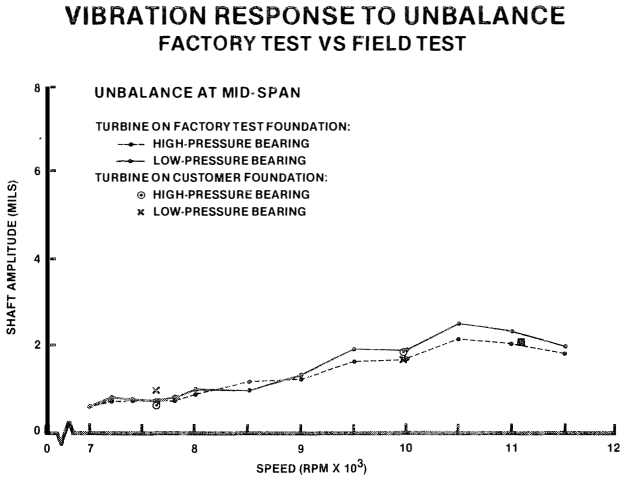

Figure 16. Response Comparison for High Speed, High Power Turbine as Tested in the Factory and in the Field. Field Data Shown at 7600, 10,000, and 11,100 RPM.

Rotor response is evaluated by calculating the forced response to unbalance versus speed. This is strongly influenced by the type of bearing used. Tilting pad journal bearings will usually give a lower response to unbalance than fixed arc bearings. The optimum number of pads and the orientation for tilting pad journal bearings is a function of the speed and the mode shape of the rotor. The actual diameter and L/D ratio is established to give a projected static journal loading between 100 to 200 psi which normally gives sufficient margin for increased loading changes due to partial arc effects as described in Section V. The best design is obtained by checking all tilting pad designs with the same unbalance, rotor geometry and support characteristics. From response versus speed curves for each configuration the best design can be chosen. For the most accurate predictions, the refinements described in Sections II and III on bearings and supports must be used.

The assumed amount of unbalance, its location, and the acceptable vibration level at the bearings are based on experience. Several locations are checked depending on the mode shape of the critical being investigated. For first criticals, the weight is placed at mid-span. The amount of unbalance is a function of the maximum speed and rotor weight.

For second criticals, the unbalance is placed at the coupling end. For double end drives, an additional calculation is made with the unbalance placed at the HP end coupling. The assumed amount of unbalance is a function of the half coupling weight as well as the speed.

In addition to response at the bearings, all close clearance points along the rotor must be checked for possible rubs at all speeds up to trip speed.

Test Procedures

Before addressing how predicted rotor response compares with actual test results, it is worthwhile to review how vibration data can be obtained to give repeatable results. Figure 17 shows the required vibration transducer arrangement for response testing. This includes a one per rev pulse generator on the rotor with a corresponding pickup, two proximity probes spaced 90° apart near the bearing at each end for relative shaft motion with respect to the bearing support bracket, and seismic probes next to each shaft relative probe to detect absolute bracket motion. The shaft probes are the non-contacting, eddy current type which are used to measure both peak-to-peak amplitude and phase relationships. With this combination of

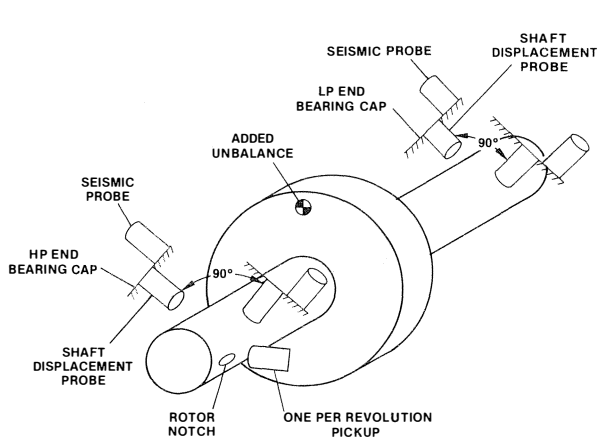

Figure 17. Schematic Sketch of Required Probe Arrangement for Testing Rotor Response to Added Unbalance.

instrumentation, absolute shaft orbits can be calculated using the shaft vibration readings relative to the bearing, and the bracket vibration readings. The amplitudes and phase angles are vectorially combined for each of the four sets of relative shaft and absolute bracket probes to obtain the absolute motion of the rotor. Many commercially available programs compute forced response to unbalance in terms of absolute shaft motion. If there is appreciable bracket motion, then the absolute shaft orbit can be significantly different from that obtained using relative shaft probes only.

Prior to the start of the test the turbine is inspected for adequate and rigid support, sufficient bearing cap pinch fit and, in the case of tilting pad journal bearings, pads which are free to follow the motion of the rotor. The journals and bearings are measured and dimensions recorded so that the actual bearing test clearances are known. The rotor has a dummy coupling attached to the driving end to simulate the overhung weight of the actual coupling in service. Experience has shown that each of the above items can have a significant effect on the amplitude of vibration and the location of criticals.

The response testing consists of two parts. The first part is the recording of filtered probe vibration data at speed points of interest. The speed range includes points around any critical and goes up to trip speed. The number and interval of points will vary depending on how many are required to adequately describe the response curve. At each speed point, at least 10 to 15 minutes will be required to allow conditions to stabilize before data is recorded. Both bearing inlet oil temperature and pressure are held steady during all testing. This first set of data defines what is called the reference run. The reference data represents rotor vibration due to residual unbalance.

To establish unbalance response, several locations are tested with unbalance weights depending on the mode shape of the critical being investigated. The amount and location of unbalance was previously described in the design analysis section.

The amount of added unbalance should be large enough to cause a sizeable (at least 2 mils) vector change in response during the unbalance run. This requirement increases the accuracy of the response test by minimizing the effects of instrumentation inaccuracies and scatter in the repeatability of test data. The amount of unbalance weight may be limited if there is a possibility of the rotor rubbing during the test. This is determined by a calculation made to check the rotor response through the entire speed range, including critical speeds that must be run through. All close clearance points along the rotor are checked for adequate running clearance, in addition to the probe and bearing centerline locations. The unbalance weight is selected to satisfy both requirements. The goal is to get accurate data for comparison with predicted results. The speed points recorded during the unbalance run correspond to those used during the reference test.

True response to unbalance can now be determined by vectorially subtracting the reference-run filtered readings (amplitude and phase) from the unbalance-run readings. The vector changes are then used to calculate orbits which are caused by the unbalance weight only. Since the residual unbalances and journal surface runouts are the same for both sets of data, their influence on response to added unbalance is nullified by looking only at vector change. This method also allows arbitrary placement of the weight circumferentially within a given unbalance plane, since for reasonable changes in vibration level the response changes in a linear fashion. If the reference run was not subtracted from the unbalance run, the resulting unbalance orbits would differ depending on whether the test unbalance weight added to or subtracted from the residual unbalance. This can be a sizeable change and would not give a true representation of rotor response.

Correlation of Analyses with Test Results

To demonstrate the correlation between calculated rotor vibration response to unbalance and measured values obtained in factory response test, two completely different turbines were selected to make the comparisons. As described in Table 2, Case I is a typical high speed, high power turbine; Case II is typical of a large, medium speed, high power turbine. Cross sections of the high speed and medium speed turbines are presented as Figures 18 and 19 to illustrate the differences in general size and geometry. A series of response tests have been run in the factory on each turbine with unbalance added at coupling and mid-span locations. The rotor dynamics analysis for each turbine includes all of the recent developments in bearing oil film analysis and the modeling of bearing support structures using impedance test data. These developments have been applied in a consistent manner to the different bearing sizes and types of bearings, sizes and types of bearing supports, and different operating conditions represented by these turbines.

The calculated and test responses for each turbine are presented in Figures 20 to 24. The correlation at each bearing has been evaluated for the operating speed ranges and also, for the first critical speed which actually occurs below minimum operating speed.

To quantify the word "correlation", the following simple convention has been adopted. The maximum calculated and test responses within the operating speed range are compared. The correlation percentage is the lesser of the two maxima

TABLE 2.

CASE I — HIGH SPEED, HIGHPOWER TURBINES (See Cross-Section, Figure 18)

TYPICAL DESIGN RANGES:

Rated Horsepowers	10,000 to 35,000 HP
Rated Speeds	7,000 to 12,000 RPM
Bearing Spans	70 to 140 IN.
Journal Diameters	4 to 8 IN.
Type of Bearings	Tilting Pad: 5 pad, load on pad 5 pad, load between pad 4 pad, load between pad

APPLICATION:

Single or double end drive, condensing turbines in compressor trains. Methanol or ammonia applications.

CASE II — MEDIUM SPEED, HIGH POWER TURBINES (See Cross-Section, Figure 19)

TYPICAL DESIGN RANGES:

Rated Horsepower	30,000 to 70,000 HP
Rated Speeds	2,000 to 6,000 RPM
Bearing Spans	160 to 230 in.
Journal Diameters	8 to 12 in.
Type of Bearings	Tilting pad: 5 pad, load on pad 5 pad, load between pad 4 pad, load between pad

APPLICATION:

Single end drive, condensing turbines in compressor trains. Ethylene or LNG applications.

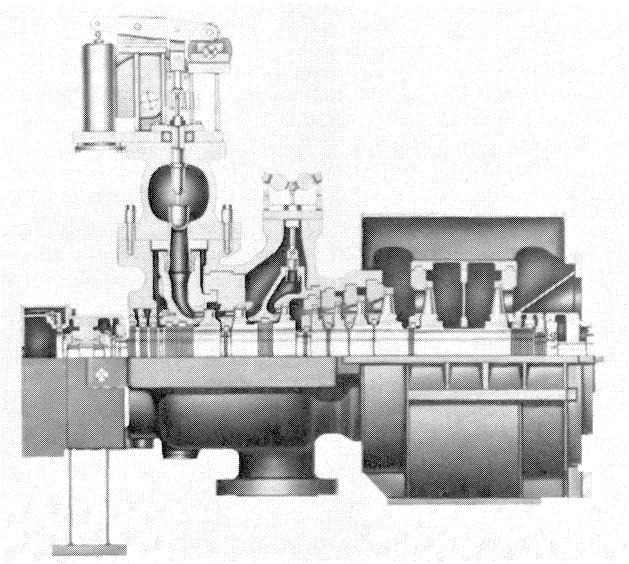

Figure 18. Cross-Section of Typical High Speed, High Power Turbine Showing Shaft Diameter, Bearing Span, and Shaft End Overhang Proportions.

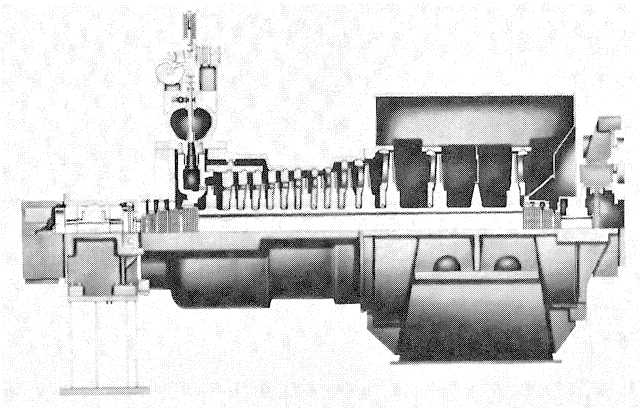

Figure 19. Cross-Section of Typical Medium Speed, High Power Turbine Showing Shaft Diameter, Bearing Span, and Shaft End Overhang Proportions.

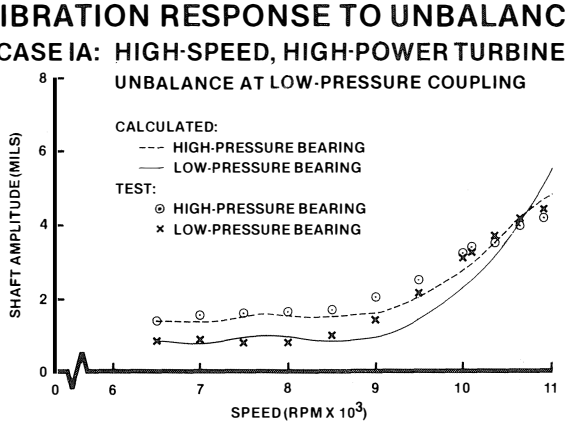

Figure 20. High Speed Turbine Rotor Vibration Response Resulting from Unbalance Added at Low Pressure Shaft End Coupling. Note Crossover in Responses near 10,500 RPM.

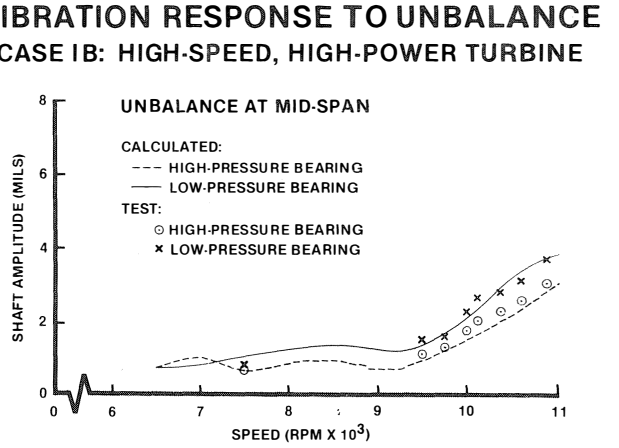

Figure 21. High Speed Turbine Rotor Vibration Response Resulting from Unbalance Added at Middle of Bearing Span.

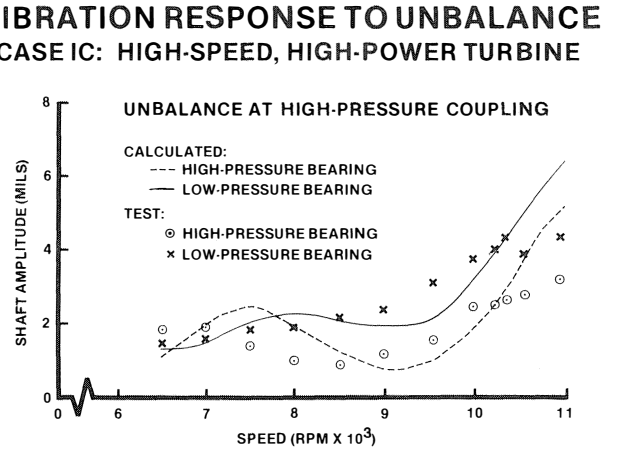

Figure 22. High Speed Turbine Rotor Vibration Response Resulting from Added Unbalance at High Pressure Shaft End Coupling.

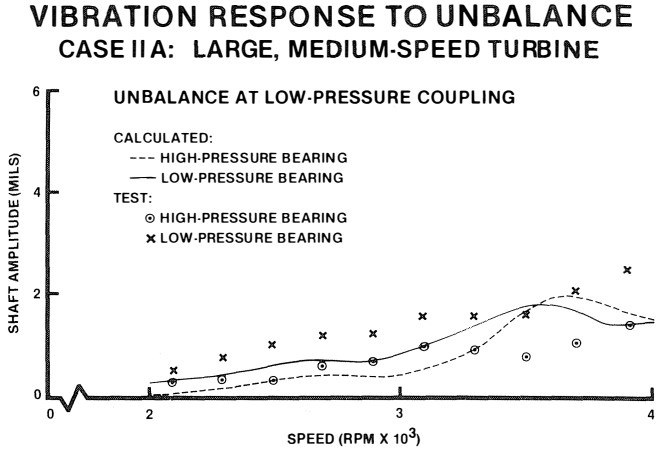

Figure 23. Medium Speed Turbine Rotor Vibration Response Resulting from Added Unbalance at Low Pressure Shaft End Coupling.

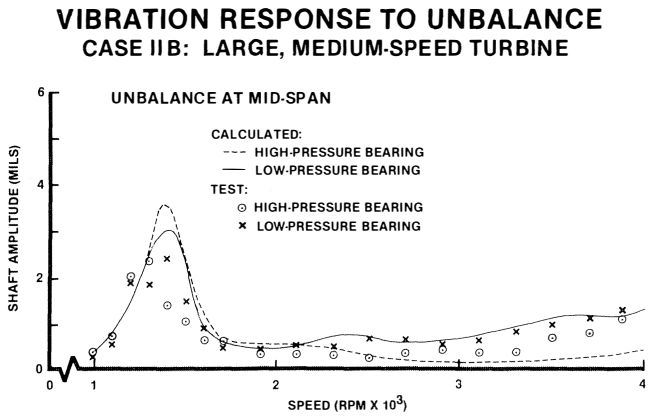

Figure 24. Medium Speed Turbine Rotor Vibration Response Resulting from Added Unbalance at Middle of Bearing Span. First Critical Speed Response Peak is Shown.

divided by the highest. For example, in Figure 20, the maximum response within the operating speed range is a calculated value of 5 mils. The maximum test response for the same added unbalance is 4.4 mils which is 88% correlation. Similarly, in Figure 23, the maximum amplitude is a test response of 2.5 mils while the maximum calculated response is 2.0 mils. The correlation, therefore, is 80%. The quantitative correlation percentages are listed in Table 3 for the different turbines and unbalance locations.

This method of evaluation has several advantages. It assumes that the maximum amplitude within the speed range is the most important consideration in the capability of predicting response. This applies whether or not there is a critical speed response within the operating speed range. Poor correlation is identified whether the actual test response is too high or too low relative to the prediction. This emphasizes the need for more realistic and consistent representations of components in the rotor dynamics system rather than arbitrary adjustments of damping or stiffness parameters to artificially force correlations. There sometimes is a tendency to consider a calculation acceptable if the actual test amplitude is less than the predicted amplitude, which implies some sort of conservatism in the calculation method. In fact, the calculation method that predicts too high is as invalid as the one that predicts too low. Furthermore, any arbitrary adjustment of parameters such as stiffness or damping will not have a consistent effect on all rotor dynamics systems. It depends on what the specific values are and the interactions between various components. For example, in Figure 15, the calculated "springs only" response correlation could be improved by adjusting the spring stiffnesses or by adding damping. This obscures the basic problem, however, which is that one or more of the system components is not properly represented. Instead, the predicted response correlation is improved by using more realistic spring-mass-damper models for support impedances. This also produces a consistent correlation at both bearings.

TABLE 3. CORRELATION OF CALCULATED VS TEST RESPONSE.

Figure	Case	Unbalance Location	Correlation %
20	IA	LP Coupling	87%
21	IB	Mid-Span	100
22	IC	HP Coupling	71
23	IIA	LP Coupling	72
24	IB	Mid-Span	95

In addition to quantitative correlations, there are qualitative aspects which must be considered. Specifically, the vibration trends over the speed range and the discrimination between responses at different bearing locations are qualitative indicators of correlation. Vibration trends pertain to the general level of vibration amplitude with changes in speed. It is possible to have excellent correlation at the maximum response speed but, at other speeds, the predicted and test responses may diverge considerably. This indicates that the correlation has been forced at maximum response speed by using artificial stiffness or damping assumptions, but it deviates at other speeds because the basic rotor dynamics model is unrealistic. Similarly, discrimination between bearing locations means that the actual relative amplitudes between bearing locations are as predicted. That is, if the calculation predicts a higher amplitude at the LP bearing than at the HP bearing, the response test should show the same relationship. The general vibration levels may be different but the relative amplitudes should have the same relationship. Another aspect of discrimination is when there is a crossover in the amplitude relationship as the speed changes. That is, the highest response may shift from one bearing location to the other. If the quantitative correlation, the vibration trends with speed, and the discrimination between bearing locations are all good, then the total rotor dynamics model is realistic.

CASE I

For the LP coupling and the mid-span unbalances (Cases IA and IB), the quantitative correlations of 87 and 100% as shown in Table 3 are excellent. In Figures 20 and 21 the vibration trends with speed are in excellent agreement both in overall magnitudes and in the relations between bearings. Note in Figure 20, the predicted and test responses both show crossovers between bearing locations near 10,500 RPM. For the HP coupling unbalance (Case IC), the quantitative correlation is 71%. The analysis predicts higher amplitudes at maximum speed than the actual test values. As Figure 22 shows, the test responses at both bearings appear more highly damped than the calculated responses as the speed approaches the 3rd critical peak. The vibration trend over the speed range and the discrimination between bearings, however, is excellent.

CASE II

With LP coupling unbalance, Case IIA, the correlation is 72% as listed in Table 3. The response comparisons in Figure 23 indicate good agreement for the vibration trends and, also, for the discrimination between bearings for speeds up to about 3300 rpm. Above this speed, the test response at the HP bearing is less than at the LP bearing while the calculated responses are about the same at both bearings.

With mid-span unbalance, Case IIB, the correlation is 95% within the operating speed range. The 1st critical response, as shown in Figure 24, occurs below minimum operating speed.

Evaluation

The quantitative percentage correlation is primarily intended to indicate whether or not further refinements or modifications are necessary in the total rotor dynamics system model or in the analytical methods.

The bearing and support component modifications described in Sections II and III have been applied in a consistent manner to both turbines. The individual effects on rotor response, however, are not necessarily consistent but are dependent primarily on the turbine size and speed. For example, the bearing changes have a much greater effect on the response of the high speed turbine than the changes in the support component. The reverse is true for the medium speed turbine. This indicates that these recent developments in bearing and support representations must be applied concurrently. The representations are more realistic than the previous simplifications and the cumulative effects produce good correlations.

The quantitative correlations in Table 3 may also indicate where further improvements might be made. In Case IC (the high speed turbine), the predicted response is greater than the test response near maximum speed. This suggests that there is an additional damping mechanism which is presently unaccounted for but may be associated with unbalance at the HP coupling of this turbine. The assumption that the thrust bearing, which is located at the HP end, has no effect on lateral rotor response could be questioned.

The complex interactions between the components in a rotor dynamics system make it essential that each component be represented with a compatible degree of sophistication. It is difficult to judge, with any certainty, what the cumulative effects of various simplifying assumptions will be on total system response. The modular approach to component analysis avoids the risk that an erroneous assumption in one component will be obscured by an equally erroneous assumption in another. If this situation exists, then acceptable correlations may be obtained for specific turbines and speeds but not for all turbines over their operating speed ranges.

PARTIAL ARC STEAM ADMISSION EFFECTS

For many years, it has been the practice of turbine designers to arrange the steam control valve opening sequence so that the first valve to open will result in a downward steam force on the rotor. The reason for this was to avoid unloading the bearings during startup conditions or low load operation which might cause undesireable rotor vibration.

It has also been recognized that the entire control valve opening sequence and the partial arc diaphragm stages must be considered; especially in cases where the partial arc steam forces are large relative to the rotor weight. [14] This could push the rotor into a sector of the bearing (Figure 25) where the dynamic characteristics of the tilting pad bearing could be significantly different from what they would be with only a vertical gravity load. The resulting rotor vibration would therefore be dependent on the turbine output; where certain loading conditions could result in significant changes in rotor response. This phenomenon would not be evident during a no load factory test evaluating response to unbalance. Only under operating conditions with load could there be cases where the partial arc force vectors are large enough to potentially shift the rotor loading in the bearing.

Force Vectors

A primary source of partial arc forces is the first stage nozzle box as illustrated in Figure 26. While, for thermal efficiency reasons, the nozzle box is sometimes constructed with a partial arc, there are other designs where there is 360° steam admission when all valves are open. Even with this configuration, however, there will be partial arc operation at partial load points with one or more valves closed. The other sources or partial arc forces are the fixed partial arc diaphragms

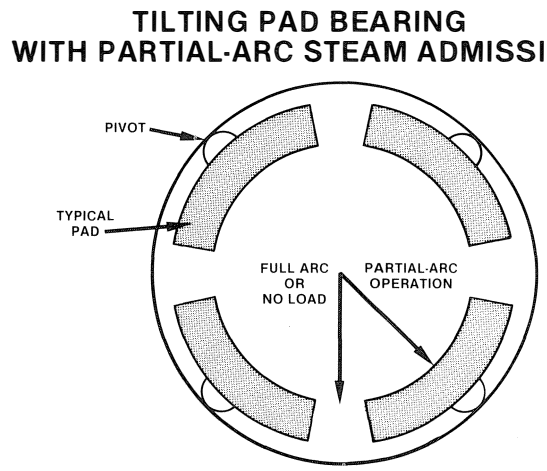

Figure 25. Rotation of Bearing Force Vector due to Effect of Partial Arc Steam Forces.

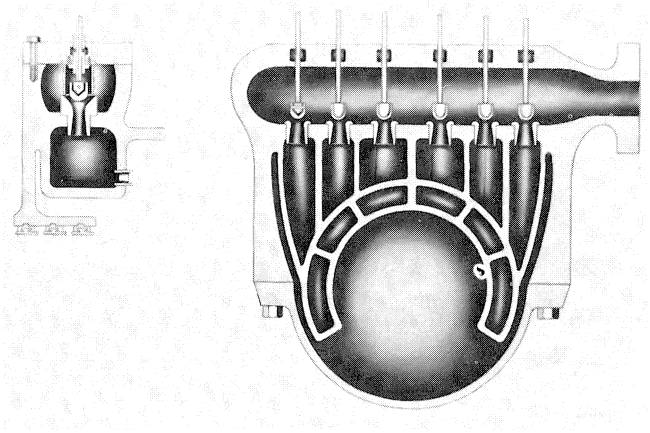

Figure 26. Cross-Section of Typical First Stage Partial Arc Nozzle Box Showing 6 Valves Controlling Steam Flow to Separate Nozzle Arcs.

that may be used in the steam path for increased efficiency. The forces on the rotor resulting from partial arcs are of two types; the lateral tangential forces which result from the torque carrying capability of the machine, and the axial thrust forces due to pressure drops across the partial arc stages. The latter forces are resolved into radial force couples at the bearing locations which are oriented at the centroids of the arcs. The tangential forces act in the same direction at both bearings.

The impact of partial arc forces on the bearings can be illustrated graphically by a force vector polar plot as shown in Figure 27. In this particular case there are six valve ports totalling 180° steam admission. The order of opening is as indicated in the figure. The plot assumes operation with the first two valves open and a maximim inlet pressure condition. While, in most cases, the thrust forces are small relative to the tangential torque forces, they are significant here because the pressure drop across the first stage is high. This produces a significant bucket axial thrust which is resolved into a radial force couple at the bearings in a nearly vertical direction. The thrust force at the bearings is normal to the torque force. The solid lines show the gravity, torque and thrust forces on the high pressure bearing which result in a change of approximately 60° for the resultant force vector and a slight increase in force

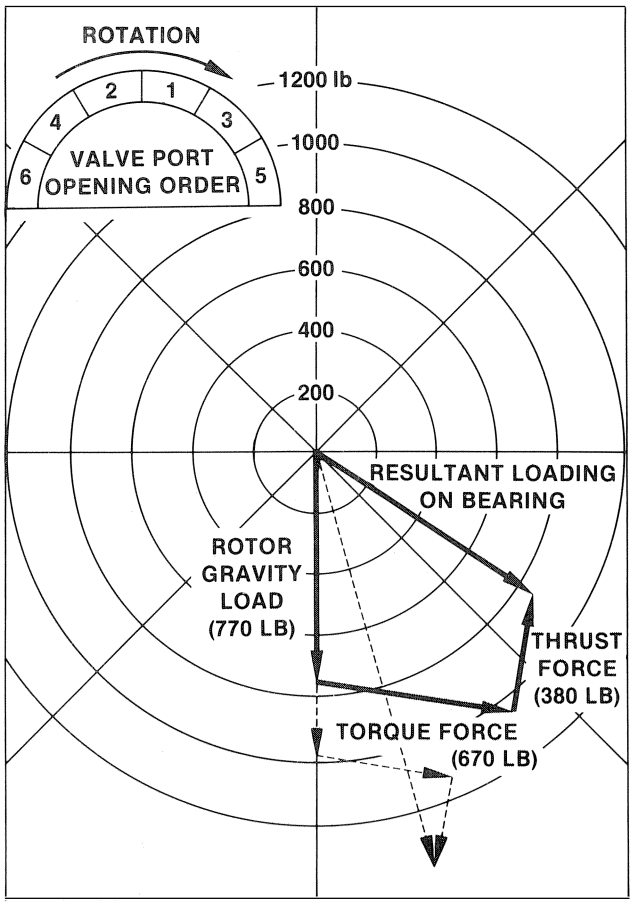

Figure 27. Resultant Bearing Load from Combined Gravity, Steam Torque, and Thrust Forces. Partial Arc Forces Result from First 2 Valves Open and Maximum Inlet Steam Pressure. Dashed Lines Show Similar Force Diagram for Other Bearing.

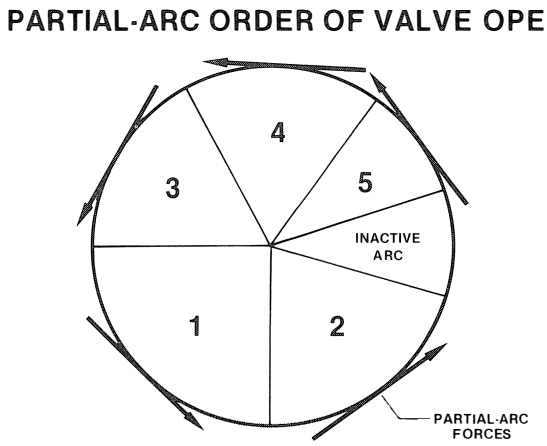

Figure 28. Nozzle Box Valve Arcs Showing Opening Sequence and Direction of Tangential Forces.

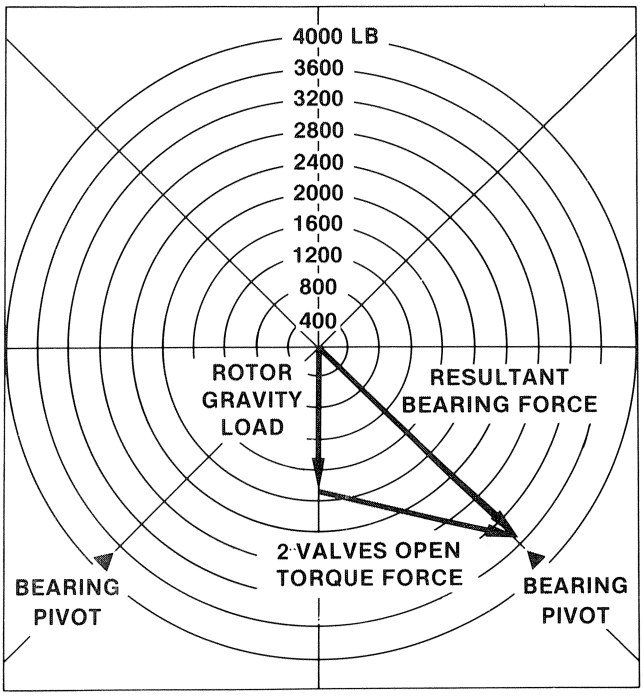

Figure 29. Resultant Bearing Load from Combined Gravity and Steam Torque Forces with 2 Valves Open at Rated Speed and Steam Conditions. Lower Half Bearing Pivot Locations Shown for 4 Pad, Load Between Pads, Bearing.

magnitude. The dashed lines show similar forces on the low pressure bearing except that the thrust force is opposite. The resultant vector angle change, therefore, is only 20°, but the magnitude is increased by 40%.

Effect on Bearing Coefficients

Field experience has verified the effects of partial arc loading on rotor response. When the partial arc steam forces are large relative to the rotor weight, the entire valve opening sequence has to be considered. The concern is that these forces can push the rotor into a sector of the bearing where the dynamic characteristics of the bearing would be significantly different from the condition without the partial arc effect. An example of this involved a small, high power non-condensing turbine in service. The sketch in Figure 28 shows the nozzle-box valve arcs with the opening sequence. The bearing was a 4-pad tilting pad bearing with the gravity load of the rotor between the pads. Figure 29 illustrates the determination of the resultant load vector on the bearing for an operating point with two valves fully opened at rated speed and steam conditions. In this particular case, the axial bucket thrust load was insignificant and it was therefore omitted. Forces are shown for only one bearing, but the axial location of the nozzle box resulted in a very similar resultant for the other bearing. It should be noted that the torque force due to the partial arc increased the bearing force to almost twice the basic gravity load on the bearing. This resulted in a resultant force vector which rotated 45° from a load between pads to a load on the pad configuration. When the rotor force vector is directed between the pads of a 4-pad bearing, the oil film stiffness and damping coefficients are nearly symmetrical. The shaft orbits are reasonably circular and well damped. When the force vector is directed toward the pad, the coefficients in line with the pad are vastly different from those that are perpendicular to the force vector. This produces a narrow, elliptical (line) orbit of much greater amplitude. Observations on a turbine in service verified that this behavior occurs.

A description of the resultant force vectors for the various

valve points at rated inlet steam pressure and speed are illustrated in Figure 30. The second valve point at rated pressure clearly was the operating point where the bearing characteristics would change significantly. The resultant force vector angle has changed 45° and the force is directly in line with the pad pivot. A 25% reduction in inlet steam pressure at the same two valve point results in lower tangential torque forces. Figure 30 shows the resultant vector angle is 30° instead of 45° for this case. This underlines the sensitivity of the partial arc effect to the steam conditions in addition to valve point, rotor weight and bearing type.

Effect on Rotor Response

A calculation showing the rotor response to unbalance at the bearing locations for the different valve points is shown in Figure 31 for the rated inlet steam pressure conditions. This shows the effect of the changing bearing stiffness and damping characteristics as the valves are opened. The bearing coefficients for the cases where the partial arc effect was not included and for the 2 valve point at rated conditions are shown in Table 4. The response change is significantly greater for the two valve condition. The bearing stiffness and damping changes resulted in increased rotor response at the rated speed. A review of Table 4 shows the 2 valve operation resulted in an increase in the direct stiffness and damping terms. Note particularly that the cross coupling terms are equivalent in magnitude to the direct terms as a result of the load vector being rotated 45° from the vertical. A comparison of the bearing coefficients for the 2 conditions shows higher stiffness and damping for the 2 valve point case. The increase in response, however, for 2 valves is not evident from the changes in stiffness and damping coefficients. This again demonstrates the fact that rotor response is a function of the total system and cannot be pre-determined with any certainty by consideration of the bearing characteristics alone.

Field data was also obtained on this particular unit. Figure 32 shows the shaft amplitude as a function of steam flow. This clearly shows a trend which is consistent with the prediction from Figure 31. Data was also obtained at a reduced inlet pressure with two valves open. A lower amplitude response was observed. This trend was also predicted from the analysis.

The high response at the second valve point was reduced by rotating the 4-pad bearing by a 25° angle in the direction of rotation (see "load vector" sketches in Figure 33). This eliminated the condition where the resulting force vector could rotate to be in line with the pivot point of the pad creating a 4-pad load on the pad configuration. A comparison of the predicted unbalance response for the various valve points at rated steam conditions and speed is given in Figure 33. A comparison with Figure 31 demonstrates the resultant insensitivity to partial arc with the rotated bearing configuration.

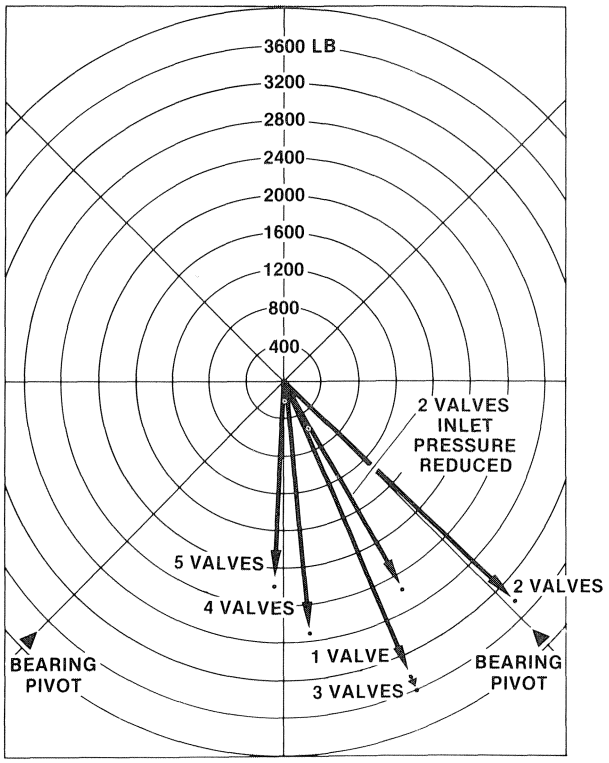

Figure 30. Resultant Force Vectors on the Bearing for Different Sequential Partial Arcs Corresponding to Number of Open Valves with Inlet Steam Pressure and Speed. Also, Resultant Force Vector with 2 Valves Open and Reduced Inlet Steam Pressure.

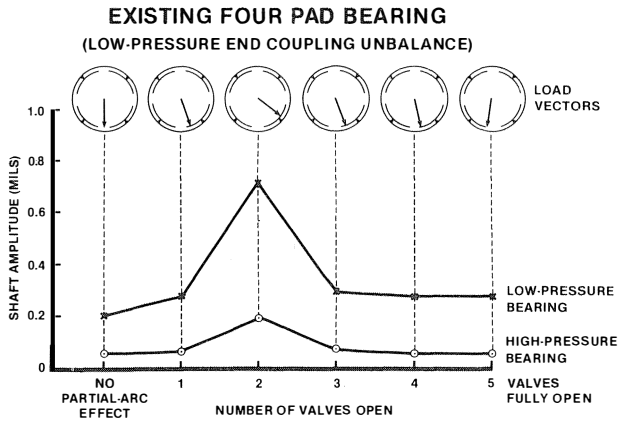

Figure 31. Calculated Rotor Response Using Bearing Coefficients Resulting from Partial Arc Vector Forces Shown in Figure 30.

TABLE 4. STIFFNESS AND DAMPING COEFFICIENT COMPARISON. NO PARTIAL ARC VS. 2 VALVE PARTIAL ARC AT RATED CONDITIONS; 4 PAD BEARING.

	HP Bearing Stiffness, 10^6 lbs./in.				HP Bearing Damping, 10^3 lbs/in./sec.			
	VV	VH	HV	HH	VV	VH	HV	HH
No Partial Arc	1.4	.02	.03	1.4	2.3	.03	.02	2.3
2 Valve Point At Rated Conditions	2.9	−2.8	−2.8	2.8	3.3	−2.8	−2.8	3.3

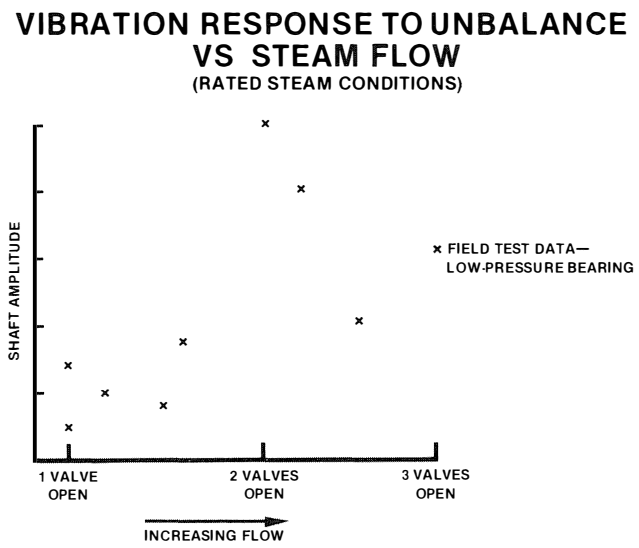

Figure 32. Field Vibration Data Showing Rotor Response at the Low Pressure Bearing Location as a Function of Steam Flow and Valve Opening.

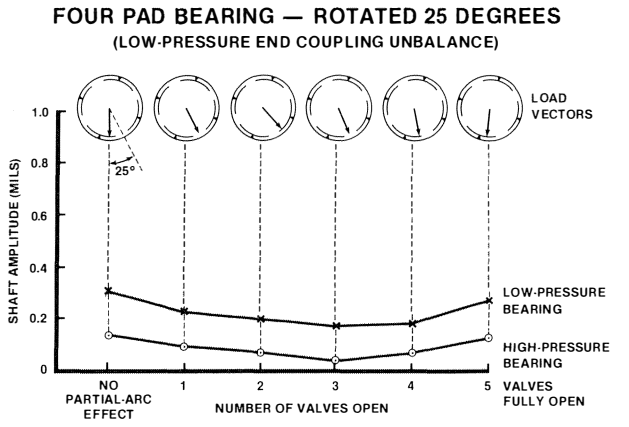

Figure 33. Calculated Rotor Response with Same Partial Arc Forces as in Figure 31 but with the Bearing Rotated 25° which Produces Different Bearing Coefficients.

Design Procedure

To avoid large changes in bearing characteristics due to force vector changes, a design procedure is used to evaluate the first stage, control valve, partial arc forces due to the valve opening sequence. Extraction valve forces are analyzed in the same way. The worst case combinations of the forces from both control stages are then identified. The effect of these forces relative to the rotor weight, the bearing loads, and the bearing type are determined.

Another aspect of the same problem occurs in conjunction with turbines that have partial arc diaphragms in the steam path, which are required for efficiency reasons. The diaphragm partial arc forces are in fixed directions but the magnitudes are proportional to steam flow. Even in some cases of longer, heavier rotors, this effect results in significant changes in the bearing loads, and can rotate the resultant rotor force vectors around toward the adjacent pad pivot points.

At the present time, the combined effects of the gravity forces and the partial arc forces (both control stages and diaphragm stages) are evaluated, and bearings are selected so that the rotation of the force vector results in acceptable rotor response and stability.

CONCLUSIONS

A. Hertzian deflections, hot preload, and oil film viscosity can cause significant changes in the calculated oil film stiffness and damping coefficients for the tilting pad bearings of variable speed turbines. The combined effects can cause reductions of 30% in stiffness and 70% in damping at high speeds. The Hertzian effect depends on the actual load-deflection characteristics of the pad pivot. Hot preload is the result of temperature gradients which exist within the bearing during operation.

B. The total bearing support structure is complex and its dynamic characteristics are difficult to predict analytically. Impedance tests provide stiffness and damping data as a function of frequency. Spring-mass-damper models are used to incorporate the test data into the rotor dynamics system.

C. The bearing forces in operating turbines include the combined effects of rotor gravity loads and steam torque reactions from control stages and from partial arc diaphragms. The steam torque reactions vary as a function of flow, inlet steam conditions, and valve lift, and, therefore, cannot be determined in a no-load factory test. The partial arc forces change the bearing oil film dynamic coefficients which can result in significant changes in rotor response and critical speed location.

D. The quantitative correlation between calculated synchronous vibration responses of rotors and the actual responses as determined by running tests has been improved by the application of state of the art developments to the rotor dynamics analysis. The qualitative correlations of vibration trends over a wide speed range and the discrimination of responses between bearing locations have also improved.

E. The increasing power density of future mechanical drive steam turbines will require greater sophistication in predicting mechanical performance. Further improvements in the rotor dynamics analyses will evolve from detailed consideration of simplifying assumptions relative to the rotor, bearing, and support components. With continuing improvements in correlation, the significance of these assumptions must be re-evaluated in terms of cumulative effects. Some specific examples are: the effects of thrust bearing restraint and damping, mechanical impedance transfer functions between bearing supports, interaction of turbine casings with rotor vibration, and the accuracy of predicted rotor mode shapes.

REFERENCES

1. W. J. Rankine, "On the Centrifugal Force of Rotating Shafts," THE ENGINEER, Vol. 27, 1869.
2. H. H. Jeffcott, "The Lateral Vibration of Loaded Shafts in the Neighbourhood of a Whirling Speed. The Effect of Want of Balance," Phil. Mag., Vol. 37, 1919.
3. M. A. Prohl, "General Method for Calculating Critical Speeds of Flexible Rotors," ASME Journ. of Appl. Mech., Vol. 12, 1945.

4. N. O. Myklestad, "A New Method of Calculating Natural Modes of Uncoupled Banding Vibration of Airplane Wings and Other Types of Beams," Journ. of Aero. Sci., Vol. 2, 1944.

5. A. C. Hagg, G. O. Sankey, "Elastic and Damping Properties of Oil-Film Journal Bearings for Application to Unbalance Vibration Calculations," J. Appl. Mech., Vol. 25, 1958.

6. J. W. Lund, "Spring and Damping Coefficients for the Tilting-Pad Journal Bearing," ASLE Trans., Vol. 7, 1964.

7. M.T.I., "Rotor-Bearing Dynamics Design Technology, Part III: Design Handbook for Fluid Film Type Bearings," Tech. Report AFAPL-TR-65-45, 1965.

8. F. C. Linn, M. A. Prohl, "The Effect of Flexibility of Support Upon the Critical Speeds of High-Speed Rotors," Soc. of Nav. Archit. & Mar. Eng., Trans., 1952.

9. W. J. Caruso, "Prediction of Critical Speeds of Steam Turbines by Dynamic Stiffness Method," Colloq. on Mech. Imped. Methods of Mech. Vibr., ASME, 1958.

10. G. M. Coleman, "Methods for the Measurement of Mechanical Impedance," Colloq. on Mech. Imped. Methods of Mech. Vibr., ASME, 1958.

11. J. C. Nicholas, R. G. Kirk, "Selection and Design of Tilting Pad and Fixed Lobe Journal Bearings for Optimum Turborotor Dynamics," Proc. of 8th Turbo Machinery Symp., Tex. A&M, 1979.

12. K. Rouch, "Dynamics of Pivot Pad Journal Bearings, Including Pad Transmission and Rotation Effects," 1982 ASLE Paper 82-Am-2E-4.

13. P. DeChondhury, E. W. Barth, "A Comparison of Film Temperatures and Oil Discharge Temperature for a Tilting-Pad Journal Bearing," ASME Paper 80-C2-Lub-37, 1980.

14. E. Pollman, H. Termuehlen, "Turbine Rotor Vibrations Excited by Steam Forces," ASME Paper 75-WA/Pwr-11, 1975.